3.5 Accretion disks: the Shakura-Sunyaev disk

3.5.1 Derivation of the disk solution

As we have seen in particular Roche lobe overflow in narrow X-ray binaries leads to the formation of accretion disks; but also in other situations the presence of disks is likely or even demonstrable. We will give here a derivation of the so-called Shakura-Sunyaev disks, one of the most simple and illustrative examples of disks.

In the derivation we will make a number of simplifications. First we assume that the disk is axially symmetric: in cylindrical coordinates r, ϕ and z we then have $\partial/\partial\phi = 0$. Further we consider stationary disks: $\partial/\partial t = 0$. We further consider here thin disks $h(r)/r \ll 1$, where h is the local thickness. Finally we assume that the viscosity in the disk is small, i.e., the resulting radial velocity $v_r \ll v_\phi$ with v_ϕ the local rotation velocity (Kepler). Further we use here Newtonian mechanics.

The law of mass conservation can be written in this case as:

$$-2\pi r \Sigma v_r = \dot{M} \tag{3.76}$$

where Σ is the mass density in the disk ($\Sigma \equiv \int_{-\infty}^{\infty} \rho dz$). For conservation of momentum in the radial direction we assume $v_r \ll v_\phi$ and therefore Kepler's law:

$$v_\phi^2 = \frac{GM}{r} \tag{3.77}$$

For conservation of angular momentum we need to take account of the viscous forces. The Keplerian rotation (3.77) implies differential rotation. Because of the different velocity at different locations there is transport of momentum etc. perpendicular to the direction of the velocity.

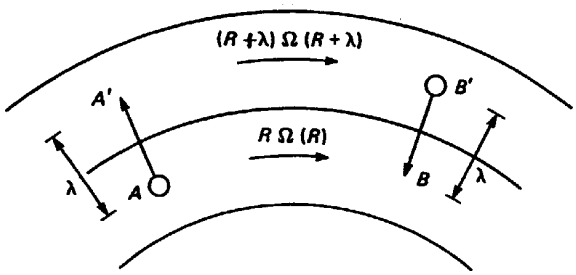

Figure 3.3: Viscous transport of angular momentum in a differentially rotating medium.

This translational viscosity (shear) must be of course zero if there is no differential rotation. Now consider the situation as indicated in Fig. 3.3. Because of the turbulent velocities $\tilde{v}$ mass elements A and B^1 move over a typical distance λ to A^1 and B. Element A brings its ϕ-velocity $\Omega(r)r$ to A^1, where it contributes $(r+\lambda)r\Omega(r)$ to the specific angular momentum of the outermost gas shell. Also B^1 adds $r(r+\lambda)\Omega(r+\lambda)$ to the specific angular momentum in the innermost shell. The net transfer of angular momentum from the inner ring to the outer ring is therefore given by $r(r+\lambda)[\Omega(r) - \Omega(r+\lambda)]$. The typical amount of mass per unit time that

contributes to this transfer of angular momentum is $2\pi r\Sigma\tilde{v}$. The total torque[1] that the inner ring exerts on the outer is therefore (with Taylor development of Ω):

$$G(r) = 2\pi r\Sigma\tilde{v}r^2\lambda\frac{d\Omega}{dr} \tag{3.78}$$

First we see that indeed for rigid rotation ($d\Omega/dr = 0$), the net transfer of angular momentum is zero, and further that for Keplerian rotation ($d\Omega/dr < 0$) the inner annulus looses angular momentum to the outer annulus. In an accretion disk every annulus (except for the innermost and outermost) has two neighbours. When a given annulus is located between r and $r + dr$, the net torque on that annulus is therefore given by $G(r + dr) - G(r) \simeq (dG/dr)dr$. The effect of this torque is that there is a net flow of matter inwards; that matter carries its own angular momentum; at the outer edge of the annulus angular momentum flows inwards in it, at the inner edge of the annulus it leaves the annulus again; in addition, there is also the local change of torque dG described above. Conservation of angular momentum therefore can be written as:

$$\frac{\partial}{\partial t}(2\pi r dr\Sigma r^2\Omega) = (2\pi r\Sigma v_r r^2\Omega)(r) - (2\pi r\Sigma v_r r^2\Omega)(r + dr) + \frac{\partial G}{\partial r}dr \tag{3.79}$$

or after Taylor development ($dr \to 0$)

$$r\frac{\partial}{\partial t}(\Sigma r^2\Omega) + \frac{\partial}{\partial r}(r\Sigma v_r r^2\Omega) = \frac{1}{2\pi}\frac{\partial dG}{\partial r} \tag{3.80}$$

In the expression for the torque (3.78) we have the characteristic turbulent free path λ and turbulent velocity $\tilde{v}$. For a thin disk the typical free path will never be much larger than the thickness h of the disk. Further, it is unlikely that the turbulent velocity $\tilde{v}$ is supersonic: in that case shocks would be produces that tend to thermalise the turbulent motions. Therefore we can write

$$\lambda\tilde{v} = \alpha c_s h \tag{3.81}$$

where $\alpha \lesssim 1$. This is the famous α-condition of Shakura and Sunyaev. The disk solution that we will find later appears to depend only weakly on α, and therefore the precise turbulent mechanism is not important. Later we will see that there are reasons to suppose that α is not very small. For cataclysmic variables one concludes based upon observations that $\alpha \sim 1$. Also magnetic turbulence (see later) can lead to a similar expression as (3.81). Therefore we have:

$$G(r) = 2\pi r\Sigma r^2\frac{d\Omega}{dr}\alpha c_s h \tag{3.82}$$

In the literature one often finds a slightly different notation. One uses

$$G(r) = -2\pi r^2 W_{r\phi} \tag{3.83}$$

where $W_{r\phi}$ is then the translational stress integrated over z:

[1]The torque vector $\mathbf{G} = \mathbf{r}\times\mathbf{F} = \mathrm{d}\mathbf{L}/\mathrm{d}t$ with $\mathbf{L} = \mathbf{r}\times\mathbf{p}$ the angular momentum, $\mathbf{p}$ the momentum and $\mathbf{F}$ the force.

$$W_{r\phi} = \int_{-\infty}^{\infty} t_{r\phi} dz \tag{3.84}$$

and where the Shakura-Sunyaev condition (3.81) is written as

$$t_{r\phi} = \alpha p \tag{3.85}$$

Both descriptions are equivalent, apart from a constant, which can be seen from the equation for pressure equilibrium in the z-direction (see later (3.93)). In the remainder of our lecture notes we will use the description (3.85).

For a stationary flow ($\partial/\partial t = 0$) it follows from (3.80) that

$$\frac{d}{dr}(r^3 \Sigma v_r \Omega) = -\frac{d}{dr}(r^2 W_{r\phi}) \tag{3.86}$$

That equation can be integrated immediately yielding (with substitution of (3.76):

$$2\Omega \dot{M} r^2 = 4\pi r^2 W_{r\phi} + C \tag{3.87}$$

where C is a constant of integration. That constant is related to the amount of angular momentum that the disk loses at its inner boundary. At the inner boundary of the disk we should have $W_{r\phi} \simeq 0$ (the disk thickness approaches zero, and for finite α, p this then follows from (3.84)). We therefore find that $C = 2\Omega_i r_i^2 \dot{M}$ where the index i indicates the inner edge of the disk. This approximation is invalid if for example the central star has a very strong magnetic field, such that it influences the mass flow through the disk until beyond the point where $\Omega_* r > (GM/r)^{1/2}$: in that case the inner edge of the disk is coupled to the rotation of the star and therefore the disk would take away energy and angular momentum from the star. If we now substitute the Keplerian angular velocity (cf. 3.77) and C into (3.87) we find

$$W_{r\phi} = \frac{\Omega \dot{M}}{2\pi}(1 - \sqrt{r_i/r}) \tag{3.88}$$

We now return to our considerations about annuli. The net torque on an annulus of thickness dr was given by $K = (\partial G/\partial r)dr$. The labour done by this torque on the rotating annulus is given by $K\Omega$. We can write this as

$$K\Omega = \Omega G' dr = [(\Omega G)' - G\Omega']dr \tag{3.89}$$

The first term represents the amount of convection of rotation energy through the gas caused by the torque; by integration over the disk one sees that this term then only depends upon the boundary conditions at the inner and outer edge of the disk. The term $G\Omega' dr$ on the other hand represents the local loss of mechanical energy to the gas. At the end that energy must be radiated at the front and rear side of the disk. Per unit of surface area the amount of dissipation Q through the disk is therefore given by

$$Q = \frac{G\Omega'}{2 \cdot 2\pi r} \tag{3.90}$$

When we substitute now $\Omega' = 0$ into this equation (solid rotation) than we see as expected that there is no dissipation. For Keplerian rotation (that we consider here) we find from (3.90) with (3.83) and (3.88) that

$$Q = \frac{3GM\dot{M}}{8\pi r^3}\left(1 - \sqrt{r_i/r}\right) \tag{3.91}$$

The energy loss of the disk is therefore independent from the precise viscosity law (it is independent of α).

EXERCISE 3.4. Show by integration that the total luminosity of the disk is given by (3.71), if the disk extends from R_* to infinity.

Half of the potential energy that the matter has lost by spiralling inwards is therefore radiated by the disk. The other half can be radiated for example in a transition layer between the disk and the neutron star.

Of the total amount of energy that is being radiated only a small part originates from the region below the surface: the dissipation per annulus is $Q \cdot 4\pi r dr = 3GM\dot{M}(1 - \sqrt{r_i/r})dr/2r^2$; only the part $GM\dot{M}dr/2r^2$ is being generated locally. The other part entered the annulus through convection from annuli that are more inwards. Demonstrate yourself that for $r \gg r_i$ this transport of energy is even two times as important as the amount of energy that is produced locally. See further Fig. 3.4.

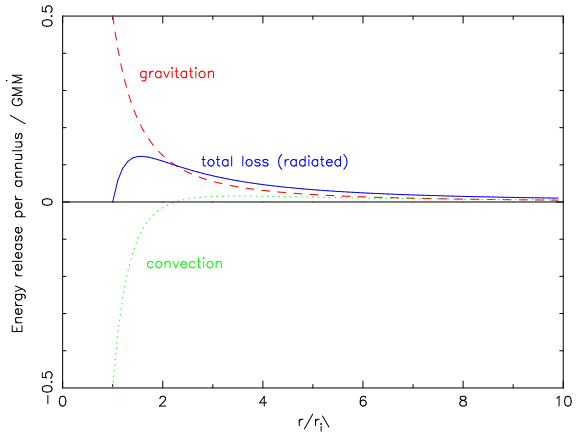

Figure 3.4: The energy losses in an accretion disk.

Finally we consider the law of momentum conservation in the z-direction. In that direction we can assume hydrostatic equilibrium: for a thin disk ($z \ll r$) this becomes (check yourself!):

$$\frac{\partial p}{\partial z} = -\frac{\rho GMz}{r^3} \tag{3.92}$$

We will not solve here in detail the structure of the disk in the z-direction. At this stage the approximation of a disk with constant density is sufficient. Note that because of symmetry we have $\partial\rho/\partial z = 0$ for $z = 0$, which justifies the zeroth-order approximation ρ =constant. Solution of (3.92) with the boundary condition $p(h) \ll p(0)$ where h is half of the total thickness of the disk then gives:

$$p(z) = \frac{\rho G M h^2}{2r^3}\,(1 - z^2/h^2) \tag{3.93}$$

Note that in this case

$$\Sigma = 2\rho h \tag{3.94}$$

and further it follows from (3.84) and (3.85) that

$$W_{r\phi} = \frac{2\rho G M h^3 \alpha}{3r^3} \tag{3.95}$$

EXERCISE 3.5. Show by integrating (3.93) that (3.95) holds.

Finally we have conservation of energy in the z-direction. We assume that the disk is optically thick; in that case we can use (3.17):

$$F(z) = -\frac{16\sigma T^3}{3\kappa_{\rm R}\rho}\frac{\partial T}{\partial z} \tag{3.96}$$

We also need the relation between pressure and temperature. We will see that apart from the gas pressure, also the radiation pressure is important in some parts of the disk. The total pressure is then given by

$$p = p_{\rm gas} + p_{\rm rad} = \frac{\rho k T}{\mu m_{\rm p}} + \frac{4\sigma}{3c}T^4 \tag{3.97}$$

We can use this relation in principle to calculate the surface flux $F(h)$. It is possible to show that in those situations where $p_{\rm gas} \gg p_{\rm rad}$ and for the constant density disk we have:

$$F(z) = \lambda \cdot \frac{4\sigma T^4 z}{3\kappa_{\rm R}\rho h^2} \tag{3.98}$$

and a similar expression holds for $p_{\rm rad} \gg p_{\rm gas}$. In gas pressure dominated situations we have $\lambda = 8$, in radiation pressure dominated situations we have $\lambda = 2$.

EXERCISE 3.6. Prove 3.98 and also prove the two values of λ mentioned in the text.

In our simple model we assumed $p(h) \ll p(0)$, and therefore we see from (3.98) together with (3.97) that in that case $F(h) \to 0$. Of course that is not realistic, and what one should do actually is to impose a full atmospheric model as a boundary condition at $z = h$. Show yourselves that for $p_{\rm rad} \gg p_{\rm gas}$ the maximum flux is given by

$$F_{\rm max} = \frac{\lambda' 4\sigma T_{\rm c}^4}{3k\rho h} \tag{3.99}$$

where $T_{\rm c}$ is the central temperature, and $\lambda' \simeq 0.77$; for $p_{\rm gas} \gg p_{\rm rad}$ we have $\lambda' \simeq 1.66$. In the following, we will choose $\lambda' = 1$. With that description we find for the law of energy conservation:

$$Q = 2F_{\rm max} \tag{3.100}$$

(the disk has 2 faces), where Q is given by (3.91). Finally, we use for $\kappa_{\rm R}$ the approximation

$$\kappa_{\rm R} = \kappa_{\rm es} + \kappa_{\rm ff} = \kappa_0 + \kappa_1 \rho T^{-7/2} \tag{3.101}$$

Further, we want to estimate the maximum value of the magnetic field in the disk. Later we come back to the importance of magnetic fields; here we only note that the energy density of the magnetic field $B^2/2\mu_0$ must be smaller than the typical turbulent energy density αp, and therefore we find:

$$B_{\rm max} = \sqrt{2\mu_0 \alpha p} \tag{3.102}$$

It is now possible to solve explicitly for the disk structure. It will become clear that in the final solution three zones can be distinguished:

1. an inner zone where $p_{\rm rad} \gg p_{\rm gas}$ and $\kappa_{\rm es} \gg \kappa_{\rm ff}$;
2. an intermediate zone where $p_{\rm rad} \ll p_{\rm gas}$ and $\kappa_{\rm es} \gg \kappa_{\rm ff}$;
3. an outer zone where $p_{\rm rad} \ll p_{\rm gas}$ and $\kappa_{\rm es} \ll \kappa_{\rm ff}$.

In our solution we will also explicitly make use of these approximations in the various zones; we then choose $\kappa_{\rm R} = \max(\kappa_{\rm es}, \kappa_{\rm ff})$ etc., For completeness we summarise here all relevant equations:

1. Mass conservation (3.76) gives v_r:
$$v_r = -\dot{M}/2\pi r \Sigma \tag{3.103}$$
2. Kepler's law (3.77) gives v_ϕ:
$$v_\phi^2 = GM/r \tag{3.104}$$
3. The definition of angular velocity gives Ω:
$$v_\phi = \Omega r \tag{3.105}$$
4. The assumption of constant thickness (3.94) gives the mass density per unit surface area Σ:
$$\Sigma = 2\rho h \tag{3.106}$$
5. Hydrostatic equilibrium in the z-direction (3.93) gives the half-thickness of the disk h (we consider here $p = p(z = 0)$):
$$p = \rho G M h^2 / 2r^3 \tag{3.107}$$
6. Further, (3.88) gives the viscous stress $W_{r\phi}$:
$$W_{r\phi} = \frac{\Omega \dot{M}(1 - \sqrt{r_i/r})}{2\pi} \tag{3.108}$$
7. On the other hand also (3.95) applies and therefore we can solve ρ:
$$W_{r\phi} = 2\rho G M h^3 \alpha / 3r^3 \tag{3.109}$$

8. The temperature follows from the pressure and density using (3.97):

$$p = \max(\rho kT/\mu m_{\rm p}, 4\sigma T^4/3c) \tag{3.110}$$

9. The opacity $\kappa_{\rm R}$ follows from the temperature and pressure with

$$\kappa_{\rm R} = \max(\kappa_0, \kappa_1 \rho T^{-7/2}) \tag{3.111}$$

10. The energy loss Q follows from (3.91):

$$Q = 3GM\dot{M}(1 - \sqrt{r_i/r})/8\pi r^3 \tag{3.112}$$

11. And finally the pressure p follows implicitly from energy conservation (3.100) by

$$Q = 8\sigma T^4/3\kappa_{\rm R}\rho h \tag{3.113}$$

12. The halve optical thickness of the disk is of course given by

$$\tau = \kappa_{\rm R}\rho h \tag{3.114}$$

13. And $B_{\max}$ by (3.102):

$$B_{\max} = \sqrt{2\mu_0 \alpha p} \tag{3.115}$$

The solution for the disk now only depends upon r, α, M and $\dot{M}$. For the solution of these equations it is handy to introduce a scaling. There are various possibilities for this. We choose here two sets of parameters: one set is suited for galactic objects, one for AGN. In both cases we will scale positions in units of GM/c^2 (half a Schwarzschild radius for a non-rotating black hole). The central mass will be scaled to 1 $\mathrm{M}_\odot$ and 10^8 $\mathrm{M}_\odot$, respectively, and the amount of accretion $\dot{M}$ will be expressed in units of 10^{14} $\mathrm{kg\,s^{-1}}$ and 10^{23} $\mathrm{kg\,s^{-1}}$ (that is 1.59×10^{-9} and 1.59 $\mathrm{M_\odot\,yr^{-1}}$). Further we write

$$f \equiv 1 - \sqrt{r_i/r} \tag{3.116}$$

Using this, we find the following scaling laws. Thereby we number the three zones with 1, 2 and 3 from the inner radius outwards. The first number always corresponds to the galactic scale, the second number to the AGN scale. See Table 3.5.1. This disk solution is the so-called Shakura-Sunyaev disk. Note that the correction factor f only occurs in combination with $\dot{M}$.

We see that in the innermost, radiation pressure dominated zone the disk height is almost constant.

EXERCISE 3.7. Show that the relative thickness of the disk h/r reaches a maximum for $r = 2.25 r_i$; for a source with $L_{\rm tot} = 2L_{\rm disk} = \frac{1}{6}\dot{M}c^2 = L_{\rm EDD}$ this gives $(h/r)_{\max} = 1.4$.

We conclude that disks are geometrically thin for $L < L_{\rm EDD}$. Further outwards the disk thickness gradually increases, through $r^{1.05}$ in the middle zone to $r^{1.125}$ in the outer zone. The mass density first increases in zone 1 with $r^{3/2}$ and then declines in the middle and outer zones. The total amount of radiation losses per unit surface area Q also shows a maximum for $r = \frac{49}{36} r_i \simeq 1.36 r_i$.

Table 3.1: The Shakura-Sunyaev disk solution. Units for M, $\dot{M}$ and r: galactic scaling: 1 $M_\odot$, 10^{14} kg s^{-1} and GM/c^2; AGN scaling: 10^8 $M_\odot$, 10^{23} kg s^{-1} and GM/c^2.

		scale			power indices			
parameter	symbol	gal.	AGN	zone	α	M	$f\dot{M}$	r
distance	r	1.48 km	1.48×10^{11} m	1–3	0	1	0	1
disk	h	1.59 km	1.59×10^{12} m	1	0	0	1	0
half		17.7 m	4.45×10^{8} m	2	-1/10	7/10	1/5	21/20
thickness		9.31 m	2.09×10^{8} m	3	-1/10	3/4	3/20	9/8
Kepler	Ω	2.03×10^{5} s^{-1}	2.03×10^{-3} s^{-1}	1–3	0	-1	0	-3/2
frequency								
period	$2\pi/\Omega$	3.1×10^{-5} s	3100 s	1–3	0	1	0	3/2
radial	r/v_r	1.27×10^{-5} s	12.7 s	1	-1	3	-2	7/2
time		0.103 s	1.63×10^{8} s	2	-4/5	8/5	-2/5	7/5
		0.124 s	2.47×10^{8} s	3	-4/5	3/2	-3/10	5/4
radial	v_r	1.16×10^{8} m/s	1.16×10^{10} m/s	1	1	-2	2	-5/2
velocity		14.4 km/s	0.908 km/s	2	4/5	-3/5	2/5	-2/5
		11.9 km/s	0.598 km/s	3	4/5	-1/2	3/10	-1/4
mass	ρ	0.0291 kg/m^3	2.91×10^{-12} kg/m^3	1	-1	1	-2	3/2
density		2.11×10^{4} kg/m^3	0.133 kg/m^3	2	-7/10	-11/10	2/5	-33/20
		4.85×10^{4} kg/m^3	0.432 kg/m^3	3	-7/10	-5/4	11/20	-15/8
surface	Σ	92.7 kg/m^2	9.27 kg/m^2	1	-1	1	-1	3/2
density		7.49×10^{5} kg/m^2	1.19×10^{8} kg/m^2	2	-4/5	-2/5	3/5	-3/5
		9.03×10^{5} kg/m^2	1.80×10^{8} kg/m^2	3	-4/5	-1/2	7/10	-3/4
total	p	1.52×10^{15} Pa	1.52×10^{7} Pa	1	-1	-1	0	-3/2
pressure		1.37×10^{17} Pa	5.44×10^{10} Pa	2	-9/10	-17/10	4/5	-51/20
		8.67×10^{16} Pa	3.87×10^{10} Pa	3	-9/10	-7/4	17/20	-21/8
pressure	$p_{\rm gas}/p_{\rm rad}$	1.31×10^{-5}	1.31×10^{-9}	1	-1/4	7/4	-2	21/8
ratio		0.0111	2.80×10^{-4}	2	-1/10	7/10	-4/5	21/20
		1.21	0.0855	3	-1/10	1/4	-7/20	3/8
central	T	4.96×10^{7} K	4.96×10^{5} K	1	-1/4	-1/4	0	-3/8
temperature		4.70×10^{8} K	2.96×10^{7} K	2	-1/5	-3/5	2/5	-9/10
		1.30×10^{8} K	6.51×10^{6} K	3	-1/5	-1/2	3/10	-3/4
surface	T_s	4.00×10^{9} K	5.17×10^{8} K	1 (MBB)	2/9	-10/9	8/9	-5/3
temperature		1.99×10^{8} K	2.21×10^{6} K	2 (MBB)	7/45	-29/45	16/45	-29/30
		5.43×10^{7} K	9.65×10^{5} K	3 (BB)	0	-1/2	1/4	-3/4
surface	Q	4.92×10^{23} W/m^2	4.92×10^{16} W/m^2	1–3	0	-2	1	-3
flux								
optical	$\tau_{\rm es}$	1.85	0.185	1	-1	1	-1	3/2
depth		1.50×10^{4}	2.37×10^{6}	2	-4/5	-2/5	3/5	-3/5
scattering		1.81×10^{4}	3.60×10^{6}	3	-4/5	-1/2	7/10	-3/4
true	$\tau^\star$	1.36×10^{-4}	4.32×10^{-7}	1	-17/16	31/16	-2	93/32
optical		0.204	1.02×10^{-7}	2	-4/5	-9/10	1/10	3/20
depth		5.61	354	3	-4/5	0	1/5	0
optical	$\tau_{\rm ff}/\tau_{\rm es}$	5.40×10^{-9}	5.40×10^{-12}	1	-1/8	15/8	-2	45/16
depth		1.50×10^{-6}	1.50×10^{-7}	2	0	1	-1	3/2
ratio		3.11×10^{-4}	9.82×10^{-5}	3	0	1/2	-1/2	3/4
maximum	$B_{\rm max}$	6.18×10^{4} T	6.18 T	1	0	-1/2	0	-3/4
magnetic		5.86×10^{5} T	370 T	2	1/20	-17/20	2/5	-51/40
field		4.67×10^{5} T	312 T	3	-9/20	-7/8	17/40	-21/16
example: zone 2, galactic scaling: $h = (17.7\text{ m})\ \alpha^{-0.1} M^{0.7} (f\dot{M})^{0.2} r^{1.05}$								

3.5.2 The inner boundary of the disk

We have not yet specified the inner edge of the disk. This inner edge can be determined by different physical processes.

The first possibility is that the disk extends up to the surface of a neutron star or white dwarf. In that case there will be a transition zone with thickness b between the stellar surface and the disk. The equation of motion in the radial direction for cylindrical symmetry in a thin disk is

$$v_r \frac{\partial v_r}{\partial r} - \frac{v_\phi^2}{r} + \frac{1}{\rho}\frac{\partial p}{\partial r} + \frac{GM}{r^2} = 0 \tag{3.117}$$

In the disk itself this equation is dominated by the second and fourth term, the centrifugal force and gravity. In the boundary layer the ϕ-component of the velocity must show a transition from the Keplerian value $\sqrt{GM/r}$ to the much lower rotation velocity of the star. In that case the gravity GM/r^2 must be compensated by the first term or the third term (pressure gradient). As an order of magnitude estimate, these terms are v_r^2/b and $c_{\rm s}^2/b$ (use here $p \sim \frac{3}{5}\rho c_{\rm s}^2$ and $\partial/\partial r \sim 1/b$). At the surfave we must have $v_r \to 0$ (by definition) and therefore close to the surface $v_r \ll c_{\rm s}$, and therefore it follows from (3.117) that

$$\frac{c_{\rm s}^2}{b} \simeq \frac{5GM}{3R^2} \tag{3.118}$$

with here R the radius of the star. In the disk we have vertical pressure equilibrium (3.92) and therefore the disk thickness h is given by (again with $p \sim \frac{3}{5}\rho c_{\rm s}^2$):

$$h^2 \sim \frac{6}{5} c_{\rm s}^2 r^3/GM \tag{3.119}$$

where we neglected here the radiation pressure. That last assumption is quite reasonable for stellar objects: for a white dwarf the innermost accretion disk zone does not exist (see Fig. 3.6 later on). From (3.118) and (3.119) together it then follows that the thickness of the transition layer is given by (see also Fig. 3.5):

$$b \simeq \frac{1}{2} h^2/R \ll h \ll R \tag{3.120}$$

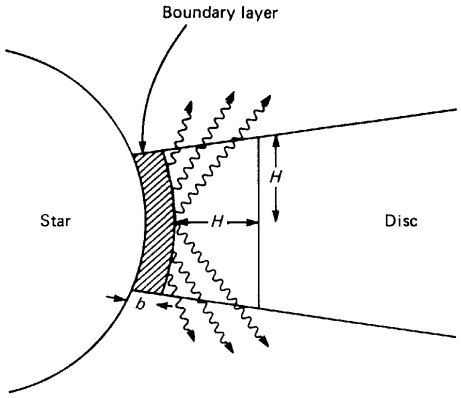

Figure 3.5: Schematic drawing of an optically thick transition layer (not to scale)

The transition layer therefore is thin compared with the thickness of the disk and the stellar radius. We can also estimate the luminosity of the transition layer. The luminosity must be equal to $\frac{1}{2}L_{\rm acc} = GM\dot{M}/2R$ (see earlier in this chapter). If we assume that the transition layer is optically thick, the spectrum is a black body. The surface of the transition layer is (see Fig. 3.5) $2\pi R \cdot 2h$. Stefan-Boltzmann's law then gives

$$4\pi R h \sigma T_{\rm bl}^4 = GM\dot{M}/2R \tag{3.121}$$

The typical maximum black body temperature follows from (3.91), for $r = \frac{49}{36}R$:

$$\frac{0.00676GM\dot{M}}{R^3} = \sigma T_{\rm d}^4 \tag{3.122}$$

Using that we find

$$\frac{T_{\rm bl}}{T_{\rm d}} \simeq 1.557\Big(\frac{R}{h}\Big)^{\frac{1}{4}} \tag{3.123}$$

For accretion onto a white dwarf one finds for typical parameters $T_{\rm bl} \simeq 10^5$ K $\simeq 3T_{\rm d}$. Some cataclysmic variables can therefore be very soft X-ray sources, where one sees mainly the transition layer at energies above ~ 0.1 keV. Observations are difficult because of the interstellar absorption (see Chapter 1). The above consideration is clearly a simplification; the strong differential rotation in the transition layer will cause additional viscosity, and moreover that layer does not need to be a priori optically thick. The presence of a hard X-ray spectrum suggests clearly a more optically thin component. In general the models for the transition layer are rather complex: we will not treat them here further.

The second possibility for the inner edge of the accretion disk we get in case of a strongly magnetised neutron star or white dwarf. In that situation one should take account of the magnetic pressure in the equations of motion. We do not give here a detailed derivation, but only give an order of magnitude estimate. When the star has a bipolar field, the field decreases as a function of radius according to

$$B \simeq m/r^3 \tag{3.124}$$

where m is the magnetic moment. The magnetic pressure is

$$B^2/2\mu_0 \tag{3.125}$$

This should be approximately equal to the ram pressure ρv^2 of the gas. We choose for this typically $\rho v_r v_\phi$ (namely the amount of mass that enters a spherical shell per second, with tangential velocity $v_\phi \gg v_r$; this v_ϕ-component must be braked). Substitution of mass conservation $\dot{M} = -4\pi r^2 \rho v_r$, and Kepler's law $v_\phi = \sqrt{GM/r}$ then gives (check yourself!):

$$r_{\rm M} = \Big(\frac{2\pi m^2}{\mu_0 \dot{M}\sqrt{GM}}\Big)^{\frac{2}{7}} \tag{3.126}$$

For a neutron star with $B = 10^8$ T and a radius of 10 km we have $m \simeq 10^{20}$ T m^3. A typical value for $\dot{M} = 10^{13}$ kg s^{-1}, and therefore the radius of the magnetosphere is 6×10^6 m, much larger than the radius of the neutron star. The quantity $r_{\rm M}$ is known as the Alfvén radius. Within $r_{\rm M}$ matter will follow the magnetic field lines towards the star. Accretion therefore mainly occurs at the magnetic poles, where the magnetic field penetrates the stellar surface. There it is possible to produce shocks, and an accretion column can exists. We will not treat here further that interesting physics. We only mention that a certain type of cataclysmic variables, the so-called AM Hercules (polar) systems, have such a large magnetosphere that an accretion disk is fully absent. The secondary component therefore touches the magnetosphere of the primary.

The third possibility that we treat here is accretion onto a black hole, either of stellar mass, or a supermassive black hole in an active galactic nucleus. In that case the accretion disk can extend down to the last stable circular orbit around the black hole. In the often considered case of a non-rotating black hole that inner radius is 3 Schwarzschild radii, or $r_i = 6GM/c^2$. The disk then reaches its maximum relative thickness for $r = 13.5GM/c^2$ and has its maximum luminosity at $r \simeq 8.16GM/c^2$. As we will see later, one can often use for simple estimates where the X-ray luminosity of the disk plays a role, the estimate $r \simeq 10GM/c^2$ as the typical distance where most of the X-ray flux is being produced.

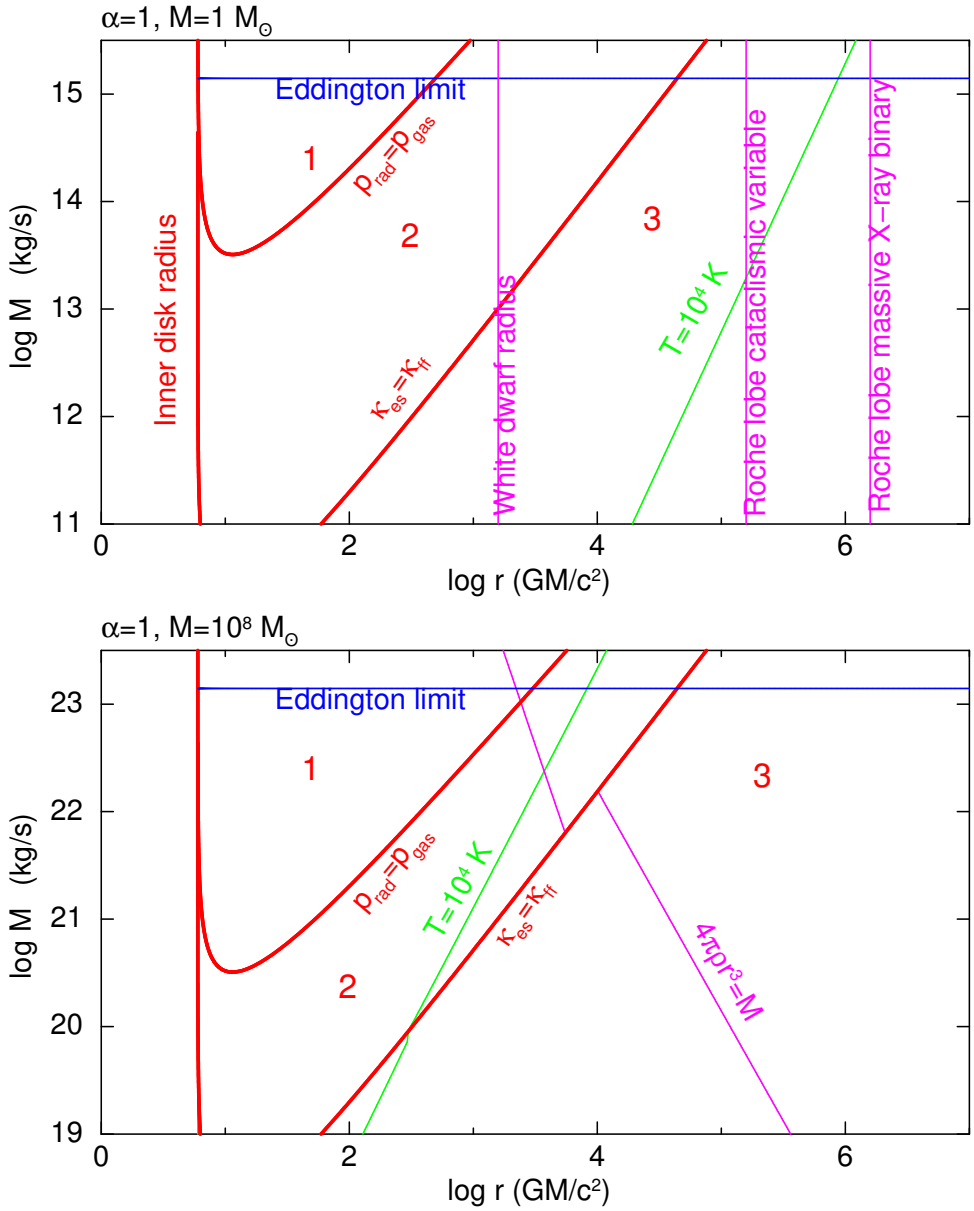

Figure 3.6: The standard Shakura-Sunyaev disk solution for a compact object of 1 $M_\odot$ (top) and 10^8 $M_\odot$ (bottom) as a function of $\dot{M}$ or L, and r. In all cases we have taken $\alpha = 1$.

3.5.3 Further consideration of the disk solution

We now return to our disk solution. In Fig. 3.6 the different regions of the solution for a black hole of 1 $M_\odot$ and 10^8 $M_\odot$ are drawn, as a function of $\dot{M}$ and r. We have chosen here the case of a non-rotating black hole as the compact object ($r_i = 6GM/c^2$).

In the inner zone the radiation pressure is much higher than the gas pressure. We see that the inner zone is larger for a larger accretion rate, and also for a higher central mass. In active galactic nuclei the role of radiation pressure is therefore more important than in stellar binary systems. In the last case, for accretion onto a white dwarf the inner zone even does not exist! In general, in the inner zone Compton scattering occurs more frequently than free-free absorption. In the middle zone this last statement still holds, but here the gas pressure gives the dominant pressure contribution. We see that this zone can be rather extended, in particular for stellar binaries. In the third, outermost region finally gas pressure and free-free absorption dominate.

Note that for $r \to r_i$ we formally find that $p_{\rm gas} \gg p_{\rm rad}$ and $\kappa_{\rm ff} \gg \kappa_{\rm es}$, which is obviously in straight conflict with what we derived before for the major part of the innermost zone. That is because in our formulae we have the factor f, that approaches 0 for $r \to r_i$. In fact, our model is not very well suited to describe the precise behaviour near to the innermost boundary. Because at that position $h \to 0$ for a finite range of r, the two-dimensional geometry that implicitly assumes that $1/h \gg \partial/\partial r$ is not valid anymore, and in principle an other, three-dimensional calculation should be done.

In the figure we further indicated the line where the central disk temperature is 10^4 K. In that region the approximation $\kappa_{\rm R} \simeq \kappa_{\rm ff}$ is definitely invalid, because there line absorption is the dominant source of opacity. We see that for binary stars that boundary is located far away in the outermost zone, but for AGN it usually is located already in the middle zone. But even already at somewhat higher temperatures, $T \simeq 10^5 - 10^6$ K, there are clearly other absorption mechanisms active, apart from free-free absorption. This can be seen easily from Chapter 1, where you can find the figure with the total Gaunt factor for *emission*, and by considering that there is a simple relation between absorption and emission coefficient, namely Kirchhoff's law:

$$j_\nu = \alpha_\nu B_\nu(T) \tag{3.127}$$

where j is the emission coefficient per steradian (W m^{-3} Hz^{-1} sr^{-1}), α the absorption coefficient (m^{-1}) and B_ν the Planck function. In particular thermal free-bound absorption is important for many regions in the disk around active galactic nuclei. See also Fig. 3.7.

Furthermore, the self gravity of the disk can play an important role, and then in particular (exclusively) in AGN. The derivation is as follows. Consider an infinitely large disks with thickness $2h$ and uniform mass density ρ. For that disk Poisson's law holds;

$$\nabla \cdot \nabla \Phi = \Delta \Phi = 4\pi G \rho \tag{3.128}$$

where

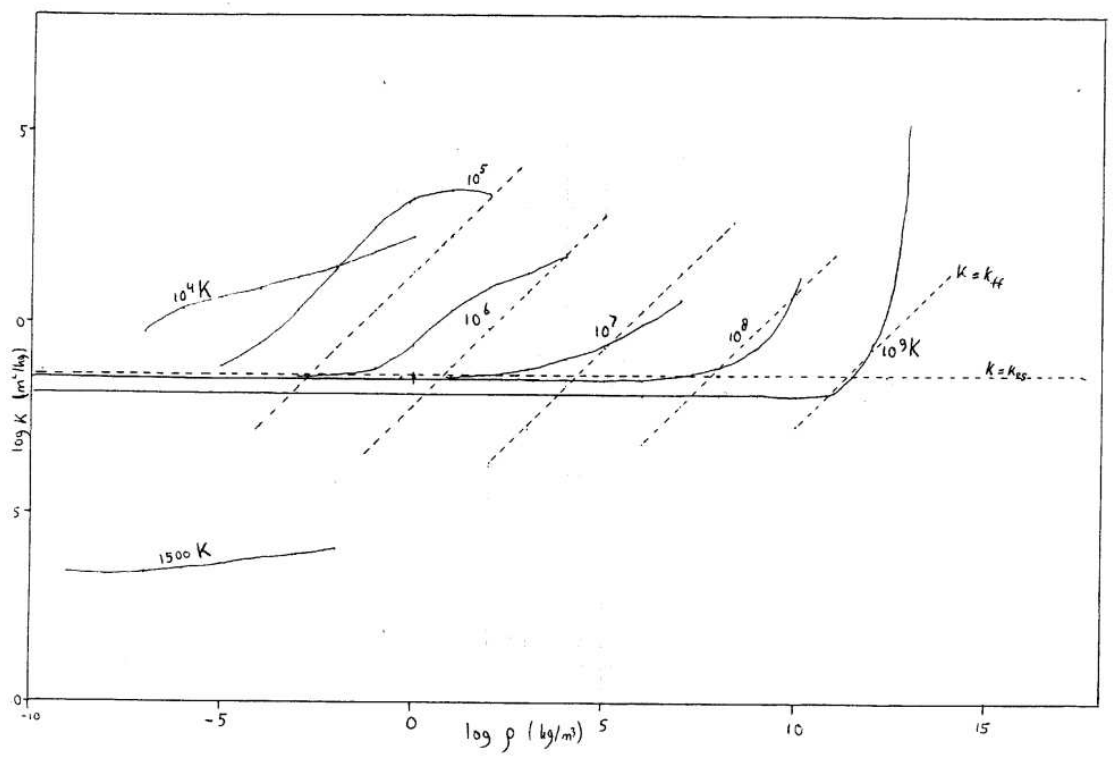

Figure 3.7: The Rosseland opacity for a cosmic plasma compared to Thomson opacity and free-free opacity, for different temperatures. The strong decline below 10^4 K is caused by the formation of H^- and He^- ions. The fact that the opacity for $T = 10^9$ K and low density is below the Thomson value is caused by Klein-Nishina effects; further, pair creation plays a role for high densities.

$$\mathbf{g} = -\nabla\Phi \tag{3.129}$$

is the gravity acceleration and Φ the potential. Now choose a small box with surface area A and thickness $2\delta z$ that is centred around the symmetry plane of the disk ($z = 0$) and with A parallel to the disk. We apply Poisson's law to that box and integrate over volume:

$$4\pi G\rho \cdot 2\delta z A = 4\pi G \int \rho dV = \int \Delta\Phi dV = \int \nabla\Phi \cdot d\mathbf{O} = -2Ag \tag{3.130}$$

We conclude that $4\pi G\rho\delta z = -g$ and therefore in general

$$g(z) = -4\pi G\rho z \tag{3.131}$$

everything of course provided $z < h$. Now for a disk where $h \ll r$ and where also $\rho(r)$ changes with the characteristic scale r, i.e., $\partial\rho/\partial r = O(\rho/r)$, we can apply the uniform flat disk approximation for the self gravity field of the disk. It is immediately clear that the equation for hydrostatic equilibrium in the z-direction must be extended to

$$\frac{dp}{dz} = -\frac{\rho G z}{r^3}(M + 4\pi\rho r^3) \tag{3.132}$$

The central mass M of the black hole is therefore corrected with the mass in the disk. In Fig. 3.6 we also show the critical radius where $4\pi\rho r^3 = M$. We see that for L close to $L_{\rm EDD}$ that boundary is located in the middle zone. In fact in that case one cannot use the solution of the middle zone, neither that one of the outer zone, but one should define a new zone where $4\pi\rho r^3 \gg M$.

EXERCISE 3.8. Demonstrate that in that new zone the disk thickness $h \sim r^{-3/10}$

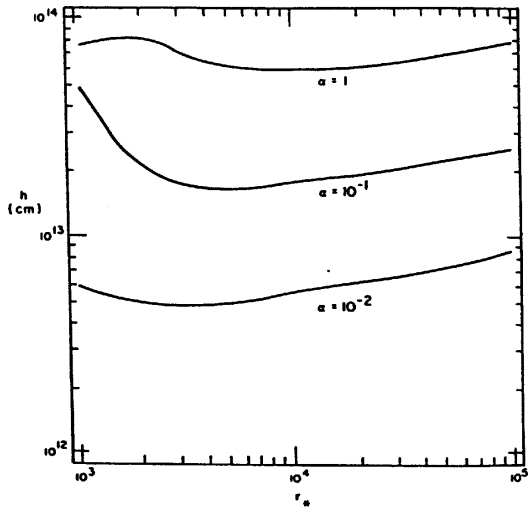

Figure 3.8: Scale height as a function of $r = r_* GM/c^2$ for the disk of a 10^8 $M_\odot$ black hole with $\dot{M} = 1$ $M_\odot$ yr^{-1} and $\alpha = 0.01$, 0.1 and 1, where the self-gravity of the disk has been taken into account.

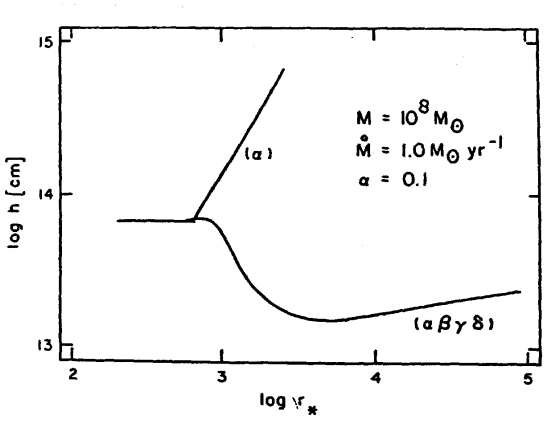

Figure 3.9: Comparison between the standard Shakura-Sunyaev disk and the disk where self-gravity has been taken into account.

We conclude that the disk becomes thinner instead of thicker if we go outwards. Therefore that zone cannot be irradiated by the central black hole. Further outwards

there will appear again a zone where $\kappa_{\rm es} \ll \kappa_{\rm ff}$ but where the self gravity of the disk still dominates; here we find $h \sim r^{9/46}$. See also Fig. 3.8 and Fig. 3.9.

The details of the solution now also depend strongly on α and $\dot{M}$. Qualitatively the scale height decreases fastest for small α and large $\dot{M}$. We mention here again that self-gravity for 1 $M_\odot$ black holes is completely negligible.

EXERCISE 3.9. Demonstrate that in the outer zone the boundary r_g for which $4\pi\rho r_g^3/M = 1$ scales as

$$r_g \sim M^{-2/3}\dot{M}^{-22/45}\alpha^{28/45}$$

when r_g is expressed in units of GM/c^2.

Finally we make here a few remarks about factors of order unity. We have already seen that at different places in the standard Shakura-Sunyaev disk theory a number of order of magnitude estimates is made. In different publications one frequently uses different constants for that. For example, the factor of 2 in the estimate of the central pressure that we made here (3.93) is not present in the original paper by Shakura and Sunyaev. Also for some of the physical constants (κ) sometime slightly different values are chosen. Whenever you find scaling laws in the literature, take care to check which basic equations have been used. Also take account of the fact that every equation that contains r^λ, after scaling scales with $r^\lambda M^\lambda$ (because here we normalise radii in units of GM/c^2). Sometimes in the literature one scales $\dot{M}$ also with $L_{\rm EDD}/c^2$ or a multiple of that; in that case one should replace the physical $\dot{M}$ by $\dot{M}M$ in the scaling law.

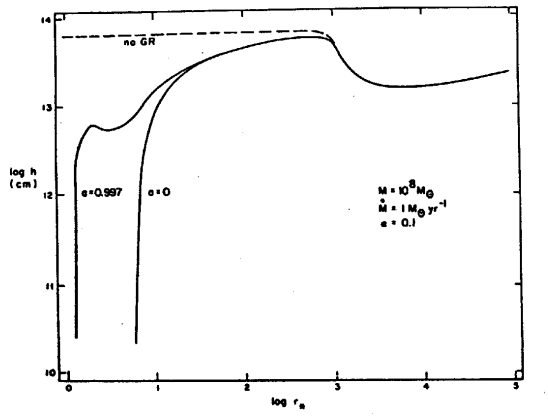

Figure 3.10: The effect of relativistic corrections on the disk thickness.

In the above we also derived the scaling laws in the Newtonian limit. It is possible to do this also correctly for the general relativistic case. See for this the paper by Novikov and Thorne (1972). One can write the basic equations in Newtonian form, with correction factors for general-relativistic effects. In order to give you an idea Fig. 3.10 shows the disk solution for h in the Newtonian, Schwarzschild and extreme Kerr limit. The curve with "no correction" gives the solution when the factor $f = 1-\sqrt{r_i/r}$ is ignored (i.e., the curve for $f = 1$). In general the difference between the Newtonian approach and the exact Schwarzschild solution is not very large. For the total disk luminosity for example Newtonian mechanics gives $L = \dot{M}c^2/12 \simeq 0.083\dot{M}c^2$, while a non-rotating black hole gives $L = (1-2\sqrt{2}/3)\dot{M}c^2 \simeq 0.057\dot{M}c^2$.

The differences with a rotating black hole are much larger: for a maximally rotating black hole the disk luminosity is $L = (1 - 1/\sqrt{3})\dot{M}c^2 \simeq 0.423\dot{M}c^2$.

3.6 The spectrum of the accretion disk

Now that we have solved the structure of the disk we can calculate the spectrum of the disk. The most simple model is obtained by assuming that the disk is optically thick everywhere and emits black body radiation. We can calculate the spectrum now very simply, because we know the total amount of radiation losses (3.91). This expression does not depend on the precise form of the viscosity law (α), and is

$$T^4 = \frac{3GM\dot{M}(1 - \sqrt{r_i/r})}{8\pi r^3\sigma} \tag{3.133}$$

We therefore see that for $r \gg r_i$:

$$T \simeq T_i(r_i/r)^{3/4} \tag{3.134}$$

where

$$T_i = \Big(\frac{3GM\dot{M}}{8\pi r_i^3\sigma}\Big)^{\frac{1}{4}} \tag{3.135}$$

For accretion with $\dot{M} = 10^{14}$ kg s^{-1} onto a 1 M$_\odot$ black hole we have $T_i = 1.4 \times 10^7$ K and for $\dot{M} = 10^{23}$ kg s^{-1} and 10^8 M$_\odot$ we have $T_i = 2.5 \times 10^5$ K. Taking into account the factor $1-\sqrt{r_i/r}$ in (3.133) we again find that T reaches a maximum for $r = \frac{49}{36}r_i$ and therefore

$$T_{\max} = 0.488T_i \tag{3.136}$$

We thus see that disks around stellar objects have radiation temperatures of at most 10^7 K and therefore they emit mainly in the hard X-ray band; while disks around AGN emit mainly in the UV and very soft X-ray band. Note that the temperature that we derived here is the radiation temperature of the surface of the disk; this should not be confused with the temperature in the symmetry plane of the disk, that is in general (much) higher.

The spectrum of a black body (in W m^{-2} Hz^{-1} sr^{-1}) is

$$I_\nu = B_\nu(T) = \frac{2h\nu^3}{c^2(e^{h\nu/kT} - 1)} \tag{3.137}$$

The total spectrum of the disk is obtained by integrating (3.137):

$$L_\nu = 2\pi\cos i \int_{r_i}^{r_o} I_\nu(r) 2 \cdot 2\pi r dr \tag{3.138}$$

The first factor of 2π is caused by the integration over half of the space (the part of the radiation that escapes outwards from the surface), the second factor 2π is caused by integration over the disk. The factor of 2 in the integral originates from the fact that the disk has two sides. Here i is the inclination of the disk, i.e. the angle between the line of sight and the normal vector to the surface. Further r_o

is the outer edge of the disk. The temperature of the disk decreases outwards; for $h_\nu \ll kT(r_o)$ we then have everywhere the Jeans approximation:

$$h\nu \ll kT(r_o): \quad L_\nu \simeq 8\pi^2 \cos i \int_{r_i}^{r_o} \frac{2kT\nu^2}{c^2} r dr = \frac{32\pi^2 r_i^2 kT_i \nu^2 \cos i}{5c^2} \Big(\frac{r_o}{r_i}\Big)^{\frac{5}{4}} \tag{3.139}$$

where we have chosen $r_o \gg r_i$ and neglected the factor $1 - \sqrt{r_i/r}$. In the other extreme case that $h\nu \gg kT_i$ the spectrum at all positions on the disk can be approximated by a Wien spectrum, and that is given by (show this!):

$$h\nu \gg kT_i: \quad L_\nu \simeq 8\pi^2 \cos i \int_{r_i}^{r_o} \frac{2h\nu^3}{c^2} e^{-h\nu/kT} r dr \sim \frac{64\pi^2 r_i^2 kT_i \nu^2 \cos i}{3c^2} e^{-h\nu/kT_i} \tag{3.140}$$

We see that the spectrum is essentially an exponentially declining function in this case; the spectrum is dominated by the hottest part $T \sim T_i$.

In the more general case we substitute $h\nu/kT = x$, so that

$$r = r_i (xkT_i/h\nu)^{4/3} \tag{3.141}$$

and therefore

$$L_\nu = \Big(\frac{64\pi^2 r_i^2 (kT_i)^{\frac{8}{3}} \cos i}{3c^2 h^{\frac{5}{3}}}\Big) \nu^{\frac{1}{3}} \int_{\frac{h\nu}{kT_i}}^{\frac{h\nu}{kT_o}} \frac{x^{\frac{5}{3}} dx}{e^x - 1} \tag{3.142}$$

We therefore see that in the domain $kT_o \ll h\nu \ll kT_i$ the spectrum is essentially proportional to $\nu^{\frac{1}{3}}$. This shape is often used to model the blue-UV excess of quasars. For an accretion disk around a black hole we also have in the mentioned domain $L_\nu \sim (M\dot{M})^{\frac{2}{3}}$. Observation of the blue-UV excess in this case leads to an estimate for $M\dot{M}$. The integral in (3.142) can be expressed in terms of the Riemann ζ-function (see Abramowitz and Stegun chapter 23):

$$\int_0^\infty \frac{x^{\frac{5}{3}} dx}{e^x - 1} = \Gamma(\frac{8}{3})\zeta(\frac{8}{3}) \simeq 1.9321\ldots \tag{3.143}$$

We are now able to summarise these findings:

$$h\nu \ll kT_o \quad : L_\nu = \tfrac{3}{10} c_1 \Big(\tfrac{T_i}{T_o}\Big)^{\frac{5}{3}} \Big(\tfrac{h\nu}{kT_i}\Big)^2 \tag{3.144}$$

$$kT_o \ll h\nu \ll kT_i \quad : L_\nu = 1.93 c_1 \Big(\tfrac{h\nu}{kT_i}\Big)^{\frac{1}{3}} \tag{3.145}$$

$$kT_i \ll h\nu \quad : L_\nu = c_1 \Big(\tfrac{h\nu}{kT_i}\Big)^2 e^{-h\nu/kT_i} \tag{3.146}$$

with

$$c_1 \equiv \frac{64\pi^2 r_i^2 (kT_i)^3 \cos i}{3h^2c^2} \tag{3.147}$$

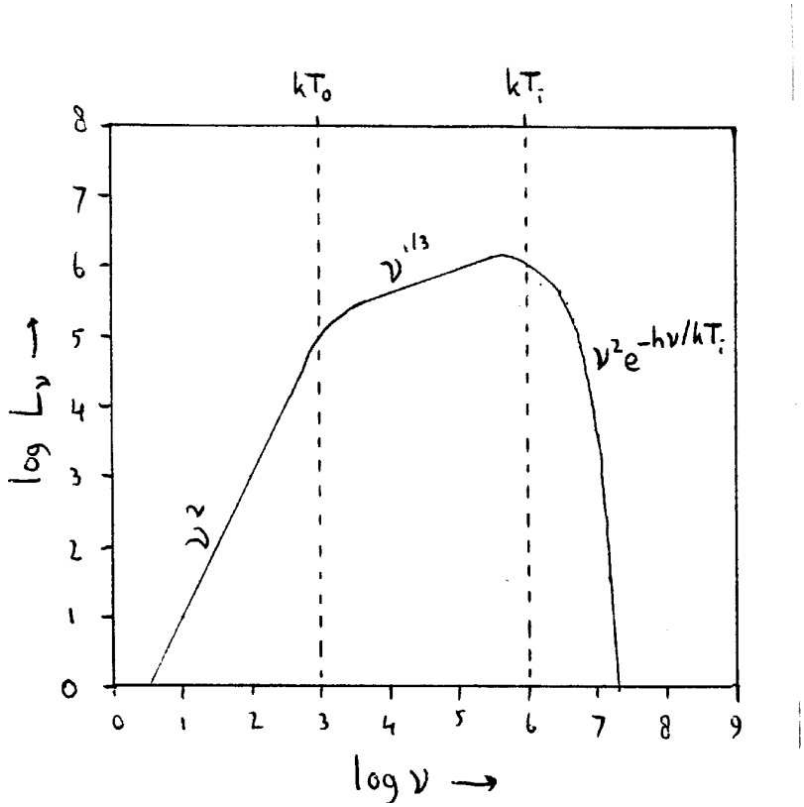

Figure 3.11: The spectrum of an accretion disk that emits locally a black body. The units along both axes are arbitrary.

The spectrum therefore goes from ν^{+2} via $\nu^{1/3}$ to an exponential spectrum (see Fig. 3.11). Note that if r_i and r_o do not differ much, the spectral zone with the intermediate $\nu^{1/3}$ spectrum is not very large.

As we will see later, the approximation of the locally emitted spectrum by a black body is not always realistic. In fact, that assumption is only justified in the outermost zone, where electron scattering plays no role. From the Shakura-Sunyaev solution we find indeed that in that outer zone $\tau_{\rm ff} \gg 1$, unless $\dot{M}$ is extremely low. In the outermost zone we therefore choose a black body radiator. The spectrum of this region is therefore described by (3.144)–(3.146), with the only difference that r_i is not the inner edge of the disk but the radius of the transition zone between the middle and outermost region, and analogously for T_i.

In the middle and inner zone we have $\kappa_{\rm es} \gg \kappa_{\rm ff}$. We now consider a photon that is produced at a given depth x, as reckoned from the surface of the disk. Would there be no scattering, then the optical depth for the photon would be $\tau_{\rm ff} = \kappa_{\rm ff}\rho x$. Most of the photons that we observe then would originate from the layer with $\tau_{\rm ff} = 1$, or from $x = 1/\kappa_{\rm ff}\rho$. Because now we have $\kappa_{\rm es} \gg \kappa_{\rm ff}$, each photon will first be scattered a number of times (say N times), before being able to reach the surface. The path of the photon therefore becomes a "drunken man's path". With N scatterings the mean distance between the point of emission and the present position of the photon is $\sqrt{N}$

times the mean distance between scatterings, which is given by $1/\kappa_{\rm es}\rho$. Therefore we find for the photons that we see:

$$y = \frac{\sqrt{N}}{\kappa_{\rm es}\rho} \tag{3.148}$$

where y is the actual depth at which most of the photons that reach us are being produced. The true path length travelled by the photon is of course given by $N/\kappa_{\rm es}\rho$. The probability of absorption (contrary to scattering) along this true path length must correspond to the optical depth for absorption that is 1, or

$$x = \frac{1}{\kappa_{\rm ff}\rho} = \frac{N}{\kappa_{\rm es}\rho} \tag{3.149}$$

The number of scatterings N is thus given by $\kappa_{\rm es}/\kappa_{\rm ff}$ and therefore it follows from (3.148) for the true emission depth y:

$$y = \frac{1}{\sqrt{\kappa_{\rm es}\kappa_{\rm ff}}\rho} \tag{3.150}$$

Therefore we can define the effective optical depth τ^* as:

$$\tau^* = \sqrt{\tau_{\rm es}\tau_{\rm ff}} \tag{3.151}$$

where $\tau_{\rm es} = \kappa_{\rm es}\rho y$ and $\tau_{\rm ff} = \kappa_{\rm ff}\rho y$. Emission then always occurs close to $\tau^* = 1$ (see (3.150)). We therefore see that in the case of an important contribution of electron scattering we must take $\tau = \tau^*$, while for negligible scattering we take $\tau = \tau_{\rm ff}$. Thus we can generalise (3.151) to:

$$\tau^* = \sqrt{\tau_{\rm ff}(\tau_{\rm es} + \tau_{\rm ff})} \tag{3.152}$$

Similar to (3.152) we can define an effective κ. The above optical depth can be determined for each frequency. The scattering opacity $\kappa_{\rm es}$ does not depend upon frequency, but $\kappa_{\rm ff}$ does depend on frequency.

EXERCISE 3.10. Demonstrate using (3.127) and the formulae for bremsstrahlung given in chapter 1 that

$$h\nu \gg kT \quad : \quad \kappa_{\rm ff} \sim \tfrac{1}{\nu^3} \tag{3.153}$$

$$h\nu \ll kT \quad : \quad \kappa_{\rm ff} \sim \tfrac{1}{\nu^2} \tag{3.154}$$

We see immediately that $\kappa_{\rm ff}$ decreases monotonically with frequency ν. From that it then follows immediately that the high-energy radiation comes from the deepest part of the disk.

At the formation point of the radiation we will have approximately $I_\nu = B_\nu$, where B_ν is the before mentioned black body spectrum. The corresponding radiation flux is $F_\nu = 2\pi B_\nu$ (half of the intensity escapes backwards, and I_ν is per steradian). But of all the photons that are emitted, only a small fraction will reach the surface; the rest is already absorbed earlier or has penetrated deeply into the disk where absorption is unavoidable.

An estimate of the final flux is obtained by assuming that all radiation generated at $\tau^* < 1$ escapes; we know that when $\tau^* = \tau_{\rm ff}$, the emitted spectrum is exactly B_ν; in our case we therefore have:

$$F_\nu = 2\pi B_\nu \frac{x}{y} = 2\pi B_\nu \sqrt{\frac{\kappa_{\rm ff}}{\kappa_{\rm es}}} \tag{3.155}$$

Now because $\kappa_{\rm es} \gg \kappa_{\rm ff}$, the flux is lower than for a black body radiator.

A more exact derivation can be found in the book of Rybicki and Lightman. The emitted intensity is given by

$$I_\nu = \frac{2B_\nu}{1 + \sqrt{(\kappa_{\rm es} + \kappa_{\rm ff})/\kappa_{\rm ff}}} \tag{3.156}$$

EXERCISE 3.11. Demonstrate that

$$\kappa_{\rm es} \ll \kappa_{\rm ff} \quad : \quad I_\nu \rightarrow B_\nu \tag{3.157}$$

$$\kappa_{\rm es} \gg \kappa_{\rm ff} \quad : \quad I_\nu \rightarrow 2B_\nu \sqrt{\kappa_{\rm ff}/\kappa_{\rm es}} \tag{3.158}$$

The total flux per unit area of the above spectrum (a so-called modified black body) is given by

$$F \simeq \sigma T^4 \sqrt{\frac{\kappa_{\rm R}}{\kappa_{\rm es}}} \tag{3.159}$$

Therefore we see that this is smaller than the flux of a simple blackbody (σT^4). In the standard disk theory however, the total emerging flux is prescribed (3.91), and therefore the surface temperature in the middle and inner zone must be higher than expected based upon a simple black body.

EXAMPLE 3.1. An accretion disk around a non-rotating black hole of 10^8 $M_\odot$ with an amount of accretion of 10^{22} kg s^{-1} (about 10 % of the Eddington limit), with $\alpha = 0.1$ in the disk, has at $r = 10GM/c^2$ a flux per surface unit of 1.1×10^{12} W m^{-2}. The equivalent black body temperature is 6.6×10^4 K. The central disk temperature is higher: 3.7×10^5 K. The disk thickness $h = 3.6 \times 10^{10}$ m, $r = 1.5 \times 10^{12}$ m. The density in the disk is $\rho = 9.2 \times 10^{-8}$ kg m^{-3}. In the disk we then find $\kappa_{\rm R}/\kappa_{\rm es} = 1.5 \times 10^{13} T^{-7/2}$. In the centre of the disk, where $T = 3.7 \times 10^5$ K, we find $\sqrt{\kappa_{\rm R}/\kappa_{\rm es}} = 7 \times 10^{-4} \ll 1$, indeed consistent with our assumption that we are here in the inner part of the disk. Using (3.159) we now find for the surface temperature 4.4×10^5 K, indeed much higher than the "black" temperature of 6.6×10^4 K.

However, a complication in this example is that the surface temperature of the disk is higher than the temperature in the midplane. This is contradictory with the earlier derived vertical pressure distribution. The cause of this discrepancy is that at this position the true optical depth τ^* is smaller than 1. In fact, at this position the spectrum is better described by optically thin, thermal emission (for example Bremsstrahlung and the other line and continuum processes of chapter 2). In the middle and inner zone of the disk we therefore can approximate the spectrum by a modified black body for $\tau^* > 1$ and an optically thin thermal spectrum for $\tau^* < 1$.

In fact, the Shakura-Sunyaev solution in the region with $\tau^* < 1$ is different from what we have derived earlier. For the radiation flux we cannot use anymore (3.17), but instead we should use (3.16). Because of this, the disk structure changes.

EXERCISE 3.12. Derive the disk structure for the inner zone (only scaling laws, no numerical constants) for $\tau^* \ll 1$. Approximate the optically thin emission with $F \sim \rho^2 T^{1/2} h$ (Bremsstrahlung).

We now consider in somewhat more detail the modified black body spectrum.

EXERCISE 3.13. Demonstrate that using the definition of Stefan-Boltzmann's constant

$$\sigma = \frac{\pi^2 k^4}{60\hbar^3 c^2} \tag{3.160}$$

and (3.137) it follows that

$$F(E)dE = \frac{30\sigma T^4 \epsilon^3 d\epsilon}{\pi^4(e^\epsilon - 1)} \sqrt{\frac{\kappa_{\rm ff}}{\kappa_{\rm es}}} \tag{3.161}$$

where E is the photon energy and $\epsilon = E/kT$ is dimensionless. $F(E)$ is the flux (in $\mathrm{W\,m^{-2}\,J^{-1}}$).

For solar abundances we have (numerical constant slightly different from what we used before):

$$\kappa_{\rm es} = 0.035 \tag{3.162}$$

$$\kappa_{\rm ff}(\epsilon) = 1.34 \times 10^{21} \rho T^{-7/2} (1 - e^{-\epsilon}) \epsilon^{-3} g_{\rm ff}(\epsilon) \tag{3.163}$$

where again everything is in SI units. The free-free Gaunt factor can be approximated by:

$$\epsilon \ll 1 \quad : \quad g_{\rm ff} = \sqrt{\frac{3}{\pi}} \ln(2.25/\epsilon) \tag{3.164}$$

$$\epsilon \gg 1 \quad : \quad g_{\rm ff} = \sqrt{\frac{3}{\pi\epsilon}} \tag{3.165}$$

The above formula (3.161) only applies as far as $\kappa_{\rm ff}(\epsilon) \ll \kappa_{\rm es}$, or $E \gg E_0$ with E_0 a critical energy; for $E \ll E_0$ the local spectrum is simply described by Planck's law (black body). From (3.163) and (3.164) it then follows that for $\epsilon \ll 1$ (in the other case scattering is unimportant):

$$E_0 = 2.0 \times 10^{-12} \ln\left(\frac{2.25kT}{E_0}\right) \rho^{\frac{1}{2}} T^{-\frac{3}{4}} \tag{3.166}$$

where E_0 is in J. For the emitted spectrum we therefore have:

$$E \ll E_0 \quad : \quad F(E) \sim E^2 T \tag{3.167}$$

$$E_0 \ll E \ll kT \quad : \quad F(E) \sim E T^{1/4} \rho^{1/2} \sqrt{\ln(2.25kT/E)} \tag{3.168}$$

$$kT \ll E \quad : \quad F(E) \sim E^{5/4} \rho^{1/2} e^{-E/kT} \tag{3.169}$$

Above kT the spectrum therefore drops exponentially. We determine the surface (emission) temperature T using (3.159) and (3.91) by choosing $Q = F$. We find (see Table 3.5.1) that in the innermost region $T \sim r^{-5/3}$, and in the middle region $T \sim r^{-29/30}$. Similar to our derivation for the black body spectrum of the disk we now can show that in the middle zone the spectrum, integrated over that zone, is proportional to $E^{1/29}$ (for the derivation: approximate the local spectrum by $F = ET^{1/4}\rho^{1/2}$ for $0 \leq E \leq kT$ and $F = 0$ for $E > kT$; further choose $r_o = \infty$ and neglect the factors with f). The spectrum in the middle zone is therefore almost flat! In the same way we find that the spectrum in the inner zone is proportional to $E^{-2/5}$, until the point where it falls exponentially at $E \simeq kT_{\max}$ with $T_{\max}$ the maximum surface temperature as a function of r.

In the optically thick part of the disk (if that is present) the temperature is much higher than if it would be optically thin: the prescribed radiation flux Q must be produced in a much smaller region. This higher temperature, however, causes immediately a complication.

In the relevant region we have $\kappa_{\rm es} \gg \kappa_{\rm R}$, and therefore most photons will be scattered many times before reaching the surface. With each scattering the energy E of the photon changes slightly:

$$\frac{\Delta E}{E} = \frac{4kT - E}{m_{\rm e}c^2} \tag{3.170}$$

where $m_{\rm e}$ is the electron mass. In general we have $E, kT \ll m_{\rm e}c^2$, and therefore the relative change of E for each scattering is small. The total number of scatterings can be very large, however, and therefore the photon can gain a lot of energy during its scattering path. The determining factor here is the Compton y-parameter, that is the product of the mean energy gain per scattering (3.170) times the mean number of scatterings. One can show that for low energies ($E \ll kT$) we have:

$$y = \frac{4kT}{m_{\rm e}c^2} \max(\tau_{\rm es}, \tau_{\rm es}^2) \tag{3.171}$$

When $y \ll 1$, Comptonisation is not important; if on the other hand $y \gg 1$, then each photon that is produced can gain a lot of energy; if Comptonisation is sufficiently strong, each spectrum finally will become a Wien spectrum:

$$I_\nu = \frac{2h\nu^3}{c^2} e^{-h\nu/kT} \tag{3.172}$$

Note the difference with the Planck spectrum (3.137)!

3.7 Hot disks

As we have seen in the previous section, in some cases the optical depth at the inner edge of the disk becomes smaller than 1. In that case the disk must be much hotter, and Comptonisation plays an important role. A closer look to the physics behind the disk structure reveals the following.

In general there are two possible solution branches for the problem: one optically thin and one optically thick branch. The optically thick branch corresponds to the standard Shakura-Sunyaev solution, as we have treated it in the previous sections. In the optically thin branch one usually assumes that the ion temperature is much

higher than the electron temperature. Because of this the electrons will gain on average energy from the ions, and the electrons in turn loose their energy to the soft photons that suffer from Inverse Compton scattering. For the source of soft photons one usually chooses two possibilities: photons emitted by Bremsstrahlung in the disk, or photons produces by a cool part of the disk.

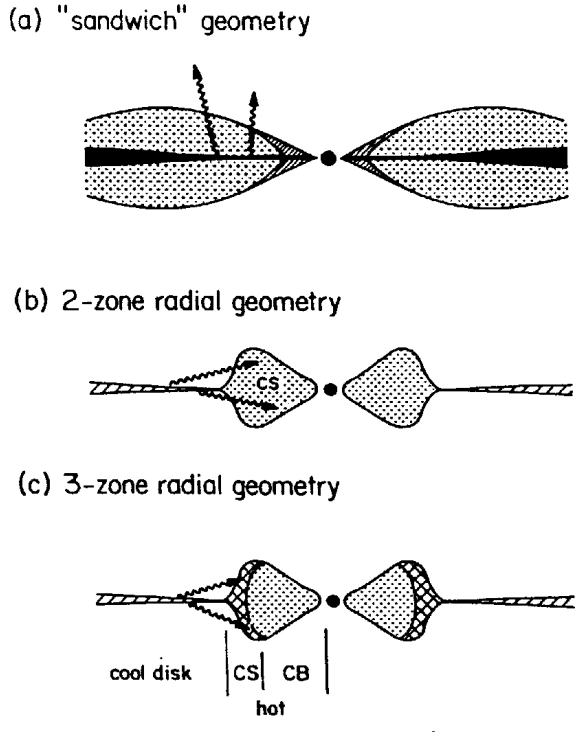

Figure 3.12: Possible different combinations of cool and hot disk solutions.

Because of the existence of two solution branches one can combine theses in different ways ("glue them together"). Fig. 3.12 shows some possibilities.

1. In the case of the *s*andwich geometry there is at every position a cool disk solution surrounded by a hot corona (optically thin). The soft photons of the disk now form the source of photons that are being scattered in the corona (only a tiny fraction will be scattered as $\tau \ll 1$).

2. In the two-zone radial geometry the outer part of the disk is relatively cool and delivers the soft photons to the hot inner part.

3. In the three-zones radial geometry the soft photons are also delivered by a cool outer disk, but the optical depth of the hot disk in the radial direction is so large, that the soft photons from the outer parts cannot penetrate the inner part. In the innermost part therefore the soft photons are locally produced by Bremsstrahlung.

The typical spectrum that is emitted by the disk is shown in Fig. 3.13. One can distinguish three components, the relative strength of those components depends upon the details of the geometry (in the figure we have chosen the three-zone geometry). The outermost, relatively cool part of the disk emits a rather soft, modified

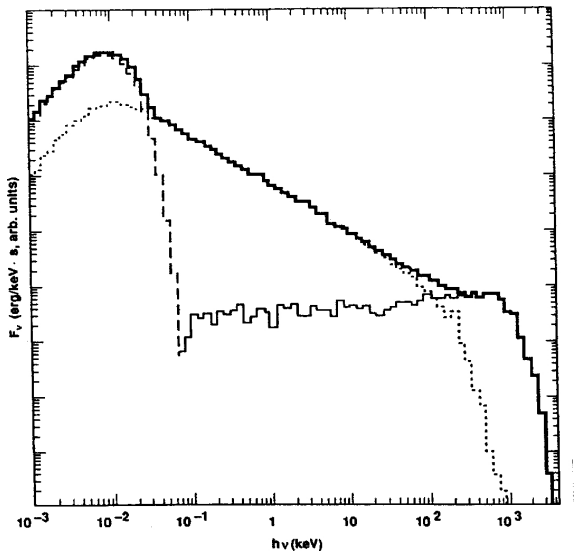

Figure 3.13: Total spectrum (thick solid line) and components of a hybrid disk (Fig. 3.12, panel c). The Comptonised Bremsstrahlung disk is located within $r < 20$ (thin continuous line), the Comptonised soft photon disk is located between $20 < r < 100$ (dotted line) and the cool disk is located at $r > 100$ (dashed line). The calculation is made for a β-disk at the Eddington luminosity. The relative luminosities of the components are here in the 3:3:1.

black body spectrum, with in this case a peak at 0.01 keV. The middle, hot zone, for which the photons are produced by the cool outer part of the disk shows an unsaturated Comptonised spectrum, that is a power law with a sharp boundary at low energies (corresponding to the mean energy of the seed soft photons), and a sharp boundary near 100 keV (corresponding to the temperature of the hot medium). Finally there is the spectrum of the innermost zone, where the photons are produced by Bremsstrahlung. Because the Bremsstrahlung spectrum is intrinsically very hard for $E \ll kT$, the Comptonised spectrum is also almost flat for energies below kT. Also here there is a sharp boundary at the temperature of the hot medium (around 1 MeV).

As an illustration we show in Fig. 3.14 the temperature profiles for the hot disk solution with Bremsstrahlung source. We see that the ion temperature cab be rather high ($10^9 - 10^{11}$ K), and in general it increases with luminosity. In the inner parts of the disk the electron temperature is much lower (sometimes even by a factor of 100), until at a given radius the electron temperature equals the ion temperature. From that point inwards both are equal.

3.8 The viscosity

Up to now we have assumed that the viscous stress scales with the total pressure (gas pressure plus radiation pressure), the so-called α-disks:

$$t_{r\phi} = \alpha(P_{\rm gas} + p_{\rm rad}) \tag{3.173}$$

Sometimes one also sees models where one assumes that the viscous stress only

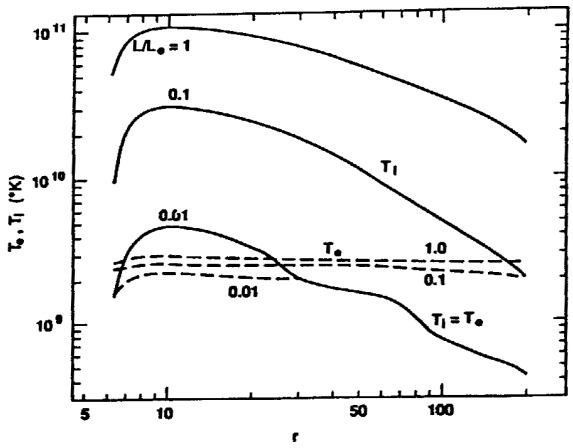

Figure 3.14: Temperature of the ions (continuous line) and electrons (dashed line) for different luminosities in a disk with Comptonised Bremsstrahlung for $\alpha = 1$ and a black hole mass of 10^8 $M_\odot$.

scales with the gas pressure, the so-called β-disks:

$$t_{r\phi} = \beta p_{\rm gas} \tag{3.174}$$

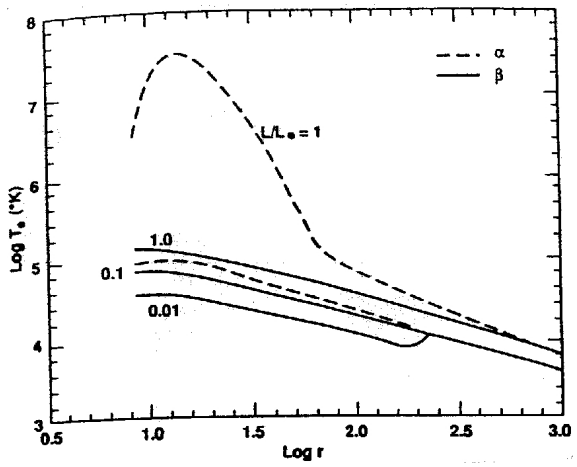

Figure 3.15: Difference between the temperature of an α-disk (dashed line) and a β-disk (continuous line).

When which condition applies exactly is not fully clear. The difference in disk structure, however, can be rather large. Fig. 3.15 shows a number of disk solutions for the same input parameters but for an α and β disk, respectively. It is clear that the α-disk is in general hotter than the β-disk. Also note that in the two outermost zones of the standard Shakura-Sunyaev disk the radiation pressure is always small as compared to the gas pressure, and therefore in those zones it does not matter whether one chooses the α or β condition.

In general one assumes that the viscosity is determined by magnetic effects. Two processes may play a role: magnetic buoyancy and reconnection.

In the case of buoyancy one considers for example a horizontal magnetic flux tube. The total pressure inside the tube is $B^2/2\mu_0 + p_{\rm gas} + p_{\rm rad}$, outside the tube it is $p_{\rm gas} + p_{\rm rad}$. If we assume that the temperatures at both sides of the tube are equal (which may be the case if the heat conduction is sufficiently efficient), then the radiation pressure at both sides is equal. Because inside the tube the magnetic pressure is higher, the density in the tube should be lower than the density of the surrounding medium, if there is pressure equilibrium between the inside and the outside of the tube. The tube therefore has a relatively low weight as compared to its surroundings, and can easily rise to reach the surface of the disk.

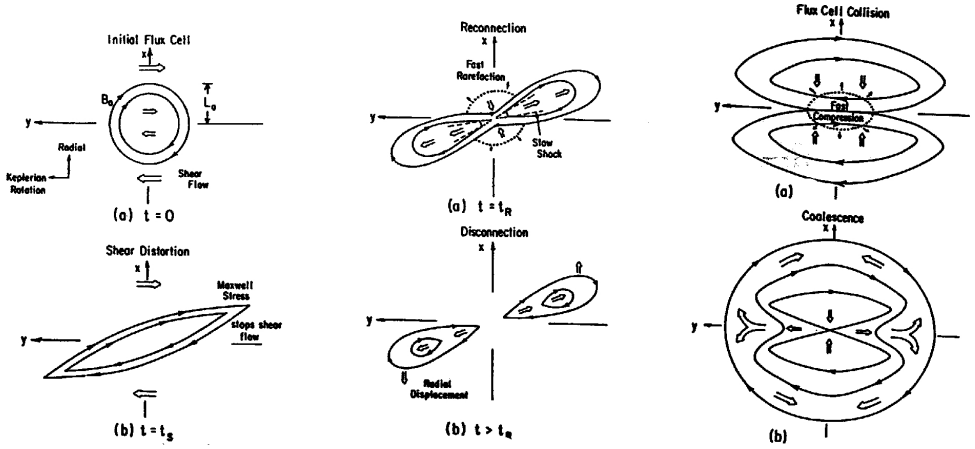

Figure 3.16: Reconnection processes in an accretion disk

Another possibility is magnetic reconnection. In Fig. 3.16 we show some stages of this process. Due to the differential rotation in the disk magnetic flux tubes are stretched, causing a rise in magnetic stress until the moment where this magnetic stress can stop locally the differential rotation. The magnetic field can relax its stress by connecting the field lines differently (reconnection). This "short circuit" (indeed high electric fields occur at the reconnection point) creates two separated flux cells. Because the flux cells do not have exactly the local Keplerian frequency, they will move slightly in the radial direction until they have the appropriate angular momentum. Both new cells in turn now can be torn apart. The entire process leads to dissipation of magnetic energy, that finally is transformed into heat and after that radiation. The process described above leads in principle to smaller and smaller flux cells. Therefore yet another process occurs, namely the collision of magnetic flux cells. Two cells of the same polarity attract each other, and at the boundary layer compression can occur, causing an increase in magnetic stress. At the boundary layer again reconnection may occur, with the corresponding dissipation of magnetic energy. The final result is that the cells merge. In practice one will get a large collection of flux cells with a broad range of scale heights, for which the condition must hold that at each scale height there is an equal number of cells that merge as that are ripped apart. The model finally can give a rough estimate for the value of the viscosity parameter, and indeed one finds that α can be of the order of $0.1 - 1$.